ARTICLES
PUBLISHED ONLINE: 27 MARCH 2017 | DOI: 10.1038/NMAT4879
nature materials

Real-time impedance monitoring of oxygen reduction during surface modification of thin film cathodes

Ghislain M. Rupp*, Alexander K. Opitz, Andreas Nenning, Andreas Limbeck and Jürgen Fleig

Improvement of solid oxide fuel cells strongly relies on the development of cathode materials with high catalytic activity for the oxygen reduction reaction. Excellent activity was found for perovskite-type oxides such as $La_{1-x}Sr_xCoO_{3-\delta}$ (LSC), but performance degradation, probably caused by surface composition changes, hinders exploitation of the full potential of LSC. This study reveals that the potentially very high activity of the LSC surface can be traced back to few very active sites. Already tiny amounts of SrO, for example, 4% of a monolayer, deposited on an LSC surface, lead to severe deactivation. Co, on the other hand, causes (re-)activation, suggesting that active sites are strongly related to Co being present at the surface. These insights could be gained by a novel method to measure changes of the electrochemical performance of thin film electrodes *in situ*, while modifying their surface: impedance spectroscopy measurements during deposition of well-defined fractions of monolayers of Sr-, Co- and La-oxides by single laser pulses in a pulsed laser deposition chamber.

Mixed ionic and electronic conducting oxides are key materials for the development of intermediate-temperature (400–600 °C) solid oxide fuel and electrolysis cells (SOFC/SOEC)[1–3]. To minimize electrical losses in such devices, oxides with high activity towards oxygen exchange are urgently needed as electrodes. Among the perovskite-type oxides, $La_{1-x}Sr_xCoO_{3-\delta}$ (LSC) is one of the most promising SOFC cathode materials, due to its potentially excellent catalytic activity for the oxygen reduction reaction (ORR) and its high oxygen diffusivity[4–9]. Surface polarization resistances as low as 0.5 Ω cm^2 were found at 600 °C in air for dense thin films[4], and this would enable sufficiently active porous electrodes at even lower temperatures. Unfortunately, those active LSC surfaces are very prone to degradation[6,10], which hinders technological exploitation of LSC's full potential as an SOFC/SOEC electrode.

Degradation of the electrochemical oxygen exchange kinetics was found for several perovskite-type materials, including $(La,Sr)MnO_{3-\delta}$ (refs 11–13), $(La,Sr)(Co,Fe)O_{3-\delta}$ (refs 6,14–17), $Sr(Ti,Fe)O_{3-\delta}$ (refs 18,19) and $(Ba,Sr)(Co,Fe)O_{3-\delta}$ (ref. 20), and was often connected to a Sr enrichment in the surface region. Moreover, ORR kinetics deteriorates strongly due to precipitates caused by contaminants in the gas phase[21,22]. The detailed mechanisms of these deactivation processes by segregates or precipitates are still unclear. Sr segregation, for example, may either passivate the entire electrode surface by forming a dense insulating SrO (or $Sr(OH)_2/SrCO_3$) layer or may block specific reactive sites important for the ORR. Degradation was even observed without a measurable change of the cation surface stoichiometry[10]. The evolution of the electrochemical performance of cathode materials is often investigated on well-defined dense thin film electrodes prepared by pulsed laser deposition (PLD). However, reported data of the initial ORR rate of as-prepared LSC thin films differ by more than three orders of magnitude[4,6,23–26]. A clear understanding of these tremendous performance differences is not available. Studies employing deliberate surface modification by a wet chemical route[27], atomic layer deposition[28] or deposition of larger amounts (several nm) of oxides via PLD (refs 29,30) shed further light on this problem but could also not resolve the exact reasons behind the variation of the ORR rates.

In this study, we show experiments revealing that LSC surfaces can be very inhomogeneous with respect to the ORR, with only rather few highly active sites, as indicated in Fig. 1. Hence, minor surface composition changes can lead to a severe performance decrease by specifically decreasing the number of highly active sites. These conclusions could be gained by employing a novel approach to investigate and modify the performance of LSC thin film electrodes. First, instead of chemical post-analysis of degraded thin film electrodes thin films, the LSC surface was deliberately changed by depositing defined amounts of its constituents. Second, surface modification and electrochemical characterization were performed simultaneously by *in situ* impedance spectroscopy during pulsed laser deposition (IPLD) of SrO, Co_3O_4 and La_2O_3 (see Fig. 2).

This avoids the disadvantage caused by the experimental decoupling of surface modification, analysis of surface changes and quantification of the electrochemical performance. The novel tool also allows us to reliably monitor small changes of the electrochemical response induced by tiny amounts of cations and to ensure that the decorated surface is not altered between modification and electrochemical characterization. Quantification of the surface deposits was performed by means of calibration measurements using inductively coupled plasma-mass spectrometry (ICP-MS). In this manner about 160 different LSC surfaces could be fabricated and analysed, and changes of the ORR kinetics could be quantitatively related to the deposited cation amount. Applying a single laser pulse onto a SrO target, for example, effectively deposits only ∼4% of a SrO monolayer on the LSC electrode surface, but already severely decreases the ORR kinetics.

$La_{0.6}Sr_{0.4}CoO_{3-\delta}$ thin film (140 nm) working electrodes were prepared on yttria-stabilized zirconia (YSZ) single crystals with a

Institute of Chemical Technologies and Analytics, Vienna University of Technology, Getreidemarkt 9, Vienna A-1060, Austria.
*e-mail: ghislain.rupp@tuwien.ac.at

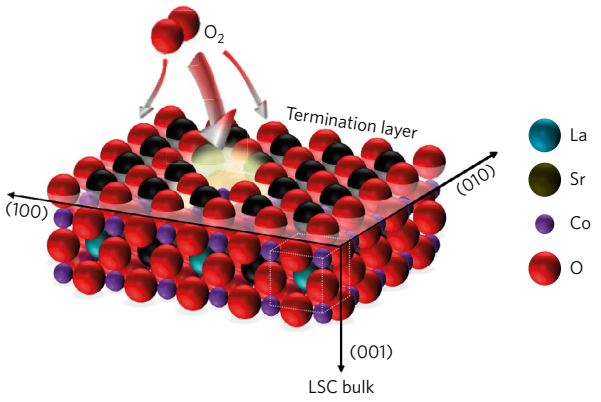

Figure 1 | Sketch of an LSC electrode with an inhomogeneously active surface for the oxygen reduction reaction (ORR). The LSC surface is largely but not completely SrO-terminated[10]; a few highly active sites, either Co itself or in the vicinity of Co, catalytically enhance the ORR.

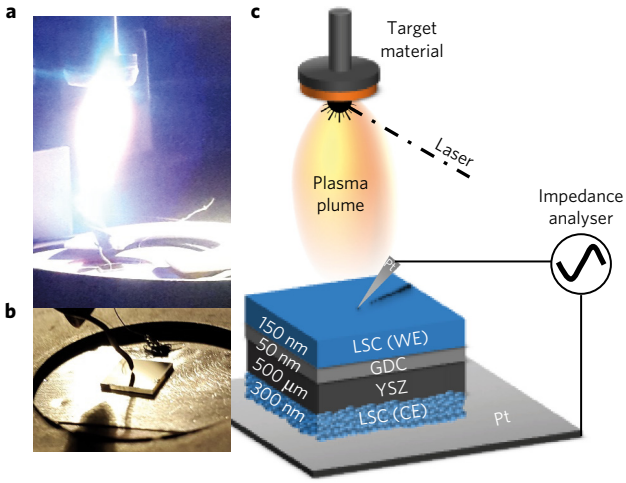

Figure 2 | The *in situ* impedance setup for PLD (IPLD). a, Setup during the ablation of target material with the sample positioned below the target and plasma plume. **b**, Sample with the macroscopic $5 \times 5\,mm^2$ dense LSC working electrode contacted by a Pt tip from above and the porous LSC counter electrode connected to a Pt sheet. **c**, Sketch of the entire setup (WE, working electrode; CE, counter electrode).

50 nm Gd-doped ceria (GDC) buffer layer. A porous LSC thin film on the bottom side of the YSZ electrolyte acted as a low-resistance counter electrode and such samples were placed on a Pt sheet in the PLD chamber. Contact to an impedance analyser was established by a Pt wire on top (see Fig. 2), thus keeping the LSC surface accessible for PLD deposition of additional oxides. This surface decoration took place at 450 °C in 0.5 mbar O_2, and hence within the stability limits of LSC[31]. The LSC working electrode surface was modified ('decorated') by applying a very limited number of laser pulses (between 1 and 888) to polycrystalline SrO ('Sr'), Co_3O_4 ('Co'), La_2O_3 ('La') and single crystalline SrO ('Sr (sc)') targets. For the deposition temperature used here, cation diffusion in LSC is sufficiently slow to avoid Sr segregation from the interior of LSC[10,32], and thus to restrict changes to the external decoration. However, surface diffusion of decorated cations is most probably still possible (see results below). Hence, our experiments mimic non-equilibrium surfaces commonly present in studies on LSC and otherwise modified by degradation. Please note that in our context 'decoration by cations' always means deposition of the corresponding electroneutral oxide.

Impedance spectra were recorded on as-prepared samples and after applying increasing numbers of PLD pulses for surface modification. Representative Nyquist plots obtained at 450 °C in 0.5 mbar O_2 after decoration by different cation amounts are shown in Fig. 3 ('Sr' and 'Co') and in Supplementary Fig. 1 ('La' and 'Sr (sc)'). The interpretation of the spectra is based on previous studies on LSC and similar mixed conducting electrodes[4,33] and is detailed in Supplementary Information. The main arc of the spectra, visible between about 100–0.01 Hz, is caused by the resistance of the oxygen exchange reaction at the working electrode surface in parallel with the bulk chemical capacitance of the LSC working electrode and was fitted to a simple R–R‖CPE equivalent circuit (see Supplementary Fig. 1). According to ref. 4 the reaction mechanism of oxygen exchange does not change when lowering the oxygen partial pressure from air to the mbar range, and hence we assume that the exchange mechanism probed in our study is the same as for LSC in air. It is, moreover, detailed in Supplementary Information that the impedance of the counter electrode does not influence the main arc.

Both as-prepared samples in Fig. 3 show a similar oxygen surface exchange resistance ($R_{surf\ exch}$) of about 250 $\Omega\,cm^2$ at 450 °C in 0.5 mbar $p(O_2)$. Decoration of the LSC surface by depositing 'Sr' or 'Co' strongly affects the ORR. Even a single pulse increases (Sr) or decreases (Co) $R_{surf\ exch}$. Such a precise relation between electrochemical response and surface modification can be monitored only by an *in situ* strategy, which ensures that the surface is not altered between preparation and measurement. $R_{surf\ exch}$ continuously increases for 'Sr' decoration, whereas it significantly decreases for 'Co'. In the latter case, however, changes level off after a few tens of laser pulses at about 30% of the original resistance values.

The same type of experiment was performed on 16 samples using four different targets for decoration and nine different amounts of laser pulses. Figure 4a displays the surface exchange resistance of all measurements on a logarithmic scale. The surface exchange resistance determined from the as-prepared samples ($254 \pm 77\,\Omega\,cm^2$) exhibits some scatter, but relative changes of each sample and also the absolute values of the complete data set reveal very clear trends. The catalytic activity for the ORR of 'Co' modified LSC surfaces was reproducibly increased by almost a factor of three after 38 pulses, corresponding to $96 \pm 17\,\Omega\,cm^2$, but then did not further change much. Decoration with 'Sr', on the other hand, leads to a strong and continuous decrease of the ORR activity with ongoing deposition: $R_{surf\ exch}$ increased by almost a factor of 100 after 888 pulses onto the polycrystalline Sr target. Deposition of 'La' shows at first no influence on the ORR activity, but after 88 pulses an increase of the surface exchange resistance is observed which, however, again decreases to nearly its initial values after 888 laser pulses.

The fact that very few pulses of 'Sr' or 'Co' may lead to severe changes of $R_{surf,exch}$ already suggests that rather small amounts of decorating oxides strongly affect the oxygen exchange kinetics (about 6,750 pulses were required to deposit the entire LSC working electrode). However, for a more quantitative discussion, knowledge on the amounts of decorating ions is essential. This was determined from a calibration series employing ICP-MS (see Methods). Hence, the deposition rates of target materials became available (6.3 pmol Co, 18.5 pmol La, 2.3 pmol Sr (sc), 12.7 pmol Sr per laser pulse). This allows us to plot the oxygen surface exchange resistance versus the amount of cations deposited on top of the LSC working electrode. From this quantitative analysis it is also possible to estimate the number of pulses required to deposit the cation amount needed for a perovskite monolayer (that is, 1.7×10^{14} cations or 283 pmol) on top of the $5 \times 5\,mm^2$ as-prepared 100-oriented LSC thin film (see also Supplementary Fig. 10).

Figure 4b displays the same resistance data as Fig. 4a but plotted versus the calculated amount of decorating cations. For all target materials, surface modifications by just a few laser pulses correspond to much less than a monolayer of the respective materials. A single laser pulse of 'Sr' equals ~4% of a

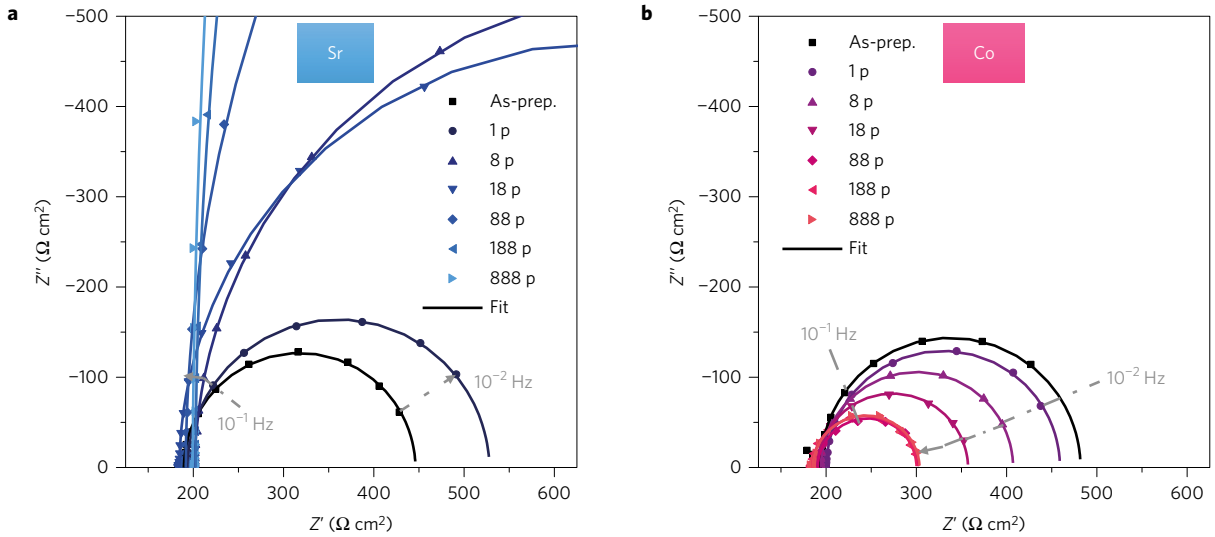

Figure 3 | Modification of impedance spectra by surface decoration. Representative Nyquist plots normalized to the surface area of the LSC working electrode of as-prepared thin films decorated with deposits from 'Sr' (**a**) and 'Co' (**b**) target measured *in situ* at 450 °C and 5×10^{-1} mbar p(O_2). The legends specify the total number of laser pulses after which the impedance spectra were recorded.

SrO monolayer (~13 pmol Sr) but still increases the initial $R_{surf\ exch}$ by about 42 ± 6%. Three pulses (~13% of a SrO monolayer) almost double $R_{surf\ exch}$. This severe detrimental effect of SrO cannot simply arise from a homogeneous passivation of the electrode surface. Rather, deposited Sr ions have to diffuse to highly active sites of an inhomogeneously active electrode surface, adhere there, and deactivate these sites. With ongoing deposition of SrO further increases of $R_{surf\ exch}$ by factors of about 6 and 11 for nominal coverages of only 23% and 53% of the LSC working electrode area, respectively, are found. This resembles the increase of the polarization resistance reported by Yu *et al.* after depositing small amounts of CeO_x by ALD on the surface of a porous LSC–YSZ composite electrode[28]. In Fig. 4c the relative resistance increase is plotted versus the Sr cation amount for 'Sr' and 'Sr (sc)' targets. The difference of both curves is statistically not significant, which shows that the difference observed between the data obtained for the two Sr targets in Fig. 4a can be attributed to the different deposition rates.

Several studies on LSC thin films, dense bulk pellets, and porous electrodes[4,6,14,21,22,27,34] found an increase of the oxygen exchange resistance with annealing time, and associated this with Sr surface segregation, measured *ex situ* on degraded samples[6,14,21,22,27]. These observations are in agreement with the deteriorating effect of SrO found in our decoration experiments. However, it was not known so far that already very small amounts of SrO can drastically poison the electrode. With this information on large effects by little Sr in mind, it is also no longer surprising that the data reported on the ORR activity of LSC scatter by orders of magnitudes; already small variations of PLD preparation conditions, annealing temperature and atmosphere, or solvents used during preparation steps, can tremendously alter the surface and thus affect the oxygen exchange kinetics. Further, such small surface stoichiometry changes may explain degradation phenomena of the electrochemical kinetics found despite the absence of measurable changes of the cation surface stoichiometry[10]. Interestingly, the negative impact of the 'Sr' deposition can still be observed after 388 laser pulses, which already corresponds to 3.3 nm of a nominally dense SrO film. This suggests that some oxygen exchange is also facilitated through SrO particles/layers, although at a much lower rate than by the active sites present at the beginning.

Decoration by one pulse of Co-oxide nominally corresponds to ~2% of a monolayer and already enhances the oxygen exchange kinetics of the LSC base film by about 13%. More pulses lead to further improvement, but the decrease of the resistance $R_{surf\ exch}$ stops after reaching a factor of three for about one Co_3O_4 monolayer. However, it should be noted that 'Co' and 'La' decorations most probably form islands on top of the electrode and do not show a layer-by-layer growth (see Supplementary Information). Additional results on the elemental composition were gathered *ex situ* on as-prepared and decorated LSC samples by X-ray photoelectron spectroscopy (XPS, see Supplementary Fig. 5). The trends of signal intensities for as-deposited surfaces and samples after 88 and 888 applied laser pulses are in accordance with the quantitative results found by ICP-MS. The Co 2*p* XPS spectra (Supplementary Fig. 6a) show similar binding energies and peak shapes for all measured samples. The Sr 3*d* spectra (Supplementary Fig. 6b) could be fitted to a surface- and a bulk-related component. The former intensity strongly increased after decorating as-deposited thin films with 'Sr (sc)' or 'Sr' (further details are given in the Supplementary Information).

The positive effect of 'Co' was further investigated on LSC films already decorated with Sr or La, and thus exhibiting higher $R_{surf\ exch}$ compared to as-prepared thin films; by 10, 30 and 80 laser pulses, up to 550 pmol Co (~1.9 monolayer of Co_3O_4), was deposited on samples first degraded by 88 pulses of 'Sr' (4.0 monolayer SrO), 'Sr (sc)' (0.7 monolayer SrO), and 'La' (5.8 monolayer La_2O_3).

For all samples a drastic improvement of the oxygen exchange kinetics by 'Co' was found (see Fig. 5). A total of 80 pulses of 'Co' was sufficient to reduce the surface exchange resistance by factors of 5.7, 18.3 and 3.4 for the samples decorated with 88 pulses of 'Sr', 'Sr (sc)' and 'La', respectively. The much stronger relative and absolute effect of the 'Co' decoration on the 'Sr (sc)' sample compared to the 'Sr' sample is most probably related to the lower deposition rate of the 'Sr (sc)' target. For the 'Sr' sample already 4.0 monolayer SrO was present and 'Co' could not improve the electrode to the same degree as for 'Sr (sc)' with only 0.7 monolayer SrO present. These and the results shown in Fig. 4b give clear experimental evidence that the accessibility of Co at the surface strongly improves the oxygen exchange kinetics. This conclusion is in agreement with findings in earlier studies[10,35]. However, also the environment of the Co may play an important role in the catalytic activity.

The following mechanistic discussion starts with the conclusion already drawn above from our results, particularly from the fact that small amounts of 'Sr' cause severe resistance increases: only relatively few surface sites of as-prepared films are highly active for

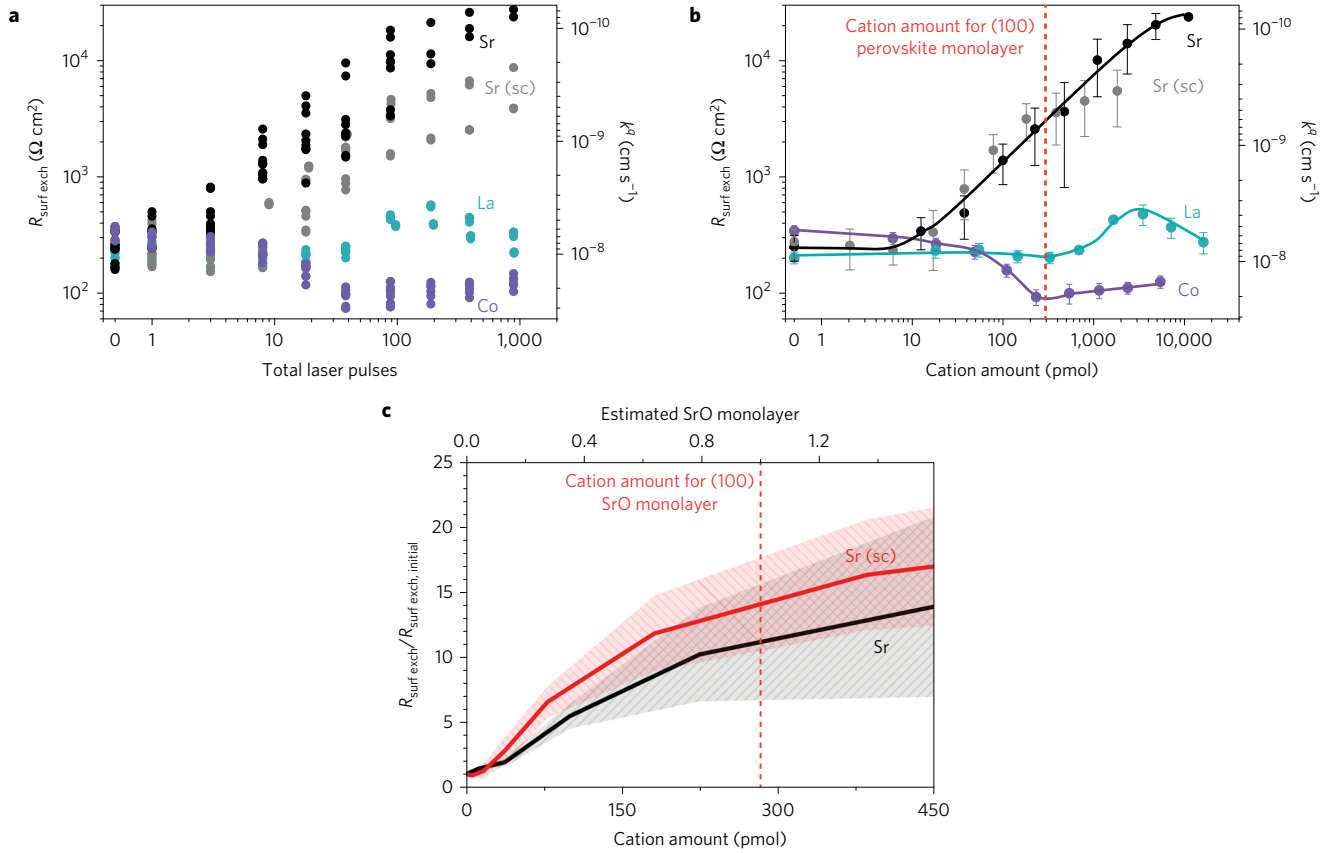

Figure 4 | Changes of the $R_{surf\ exch}$ after decorating as-deposited LSC thin films with different materials in the IPLD setup. a, Dependence of the surface exchange resistance and surface exchange coefficient k^q on the number of laser pulses used to decorate the LSC working electrode surface of 16 samples at 450 °C in 5×10^{-1} mbar p(O_2). **b**, Surface exchange resistance plotted versus the amounts of cations deposited on the LSC working electrode surface (log–log plot, lines are guides to the eye); the surface exchange coefficient k^q plotted on the right ordinate is not an independent quantity but can be simply calculated from the measured $R_{surf\ exch}$ by[37] $k^q = RT/(4F^2 R_{surf\ exch} c_O)$ with R being the gas constant, T the absolute temperature, F Faraday's constant, and c_O the oxygen lattice site concentration in LSC. The nominal amount of cations needed to form a (100) perovskite monolayer is indicated as well. **c**, Increase of the surface exchange resistance relative to its initial value with ongoing deposition of 'Sr' and 'Sr (sc)'. Effects of 'Sr' and 'Sr (sc)' decoration are the same within the error bars (coloured area). Error bars show the standard deviation of the mean from three samples including two to three measurements for each sample.

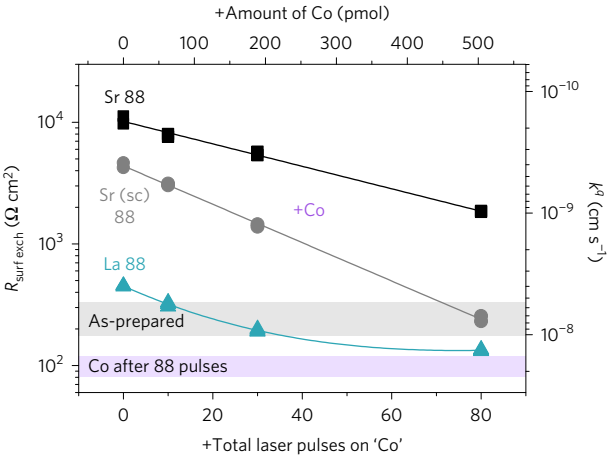

Figure 5 | Variation of the surface exchange resistance by two decorating oxides. Decrease of the surface exchange resistance of samples already decorated with 88 laser pulses of the 'Sr', 'Sr (sc)' and 'La' target after applying 10, 30 and 80 laser pulses to the 'Co' target at 450 °C in 5×10^{-1} mbar p(O_2).

oxygen exchange, and the decorating Sr cations do not randomly cover the surface but specifically deactivate these active sites. Our model of the relation between the ORR and the cation surface stoichiometry is sketched in Fig. 6 and detailed in the following.

According to a recent study[10], as-prepared LSC films as used here exhibit a kind of SrO termination (about one monolayer, black in Fig. 6a) even though some La (10%) and Co (9%) cations are still present in this surface layer. The SrO termination layer is followed by about 3 nm of Sr-enriched LSC layers, where Sr substitutes La on the A site while Co is already close to bulk stoichiometry (black-blue gradual region)[10]. We suggest that the remaining Co surface sites ('Co termination', violet in Fig. 6a) are responsible for most of the oxygen exchange activity of as-prepared LSC films and that those enable the rather low surface polarization resistance of LSC. By chemically removing the terminating SrO layer, the oxygen surface exchange resistance can be further lowered, in agreement with an enhanced Co concentration (27%)[10]. The SrO-terminated part of the film, however, is also not completely inactive, it only exhibits a much reduced oxygen exchange rate (see Fig. 6a). When depositing SrO, Sr surface diffusion to Co-termination sites takes place and almost none of these sites remain active after some 'Sr' decoration (see Fig. 6b). Possibly, the 'Co-termination' sites are primarily located at extended surface defects such as edges, and Sr preferably attaches to these sites.

After deactivating all Co sites, only the much slower oxygen exchange via SrO-terminated regions remains possible. Deposition of additional SrO then 'only' increases the thickness of the

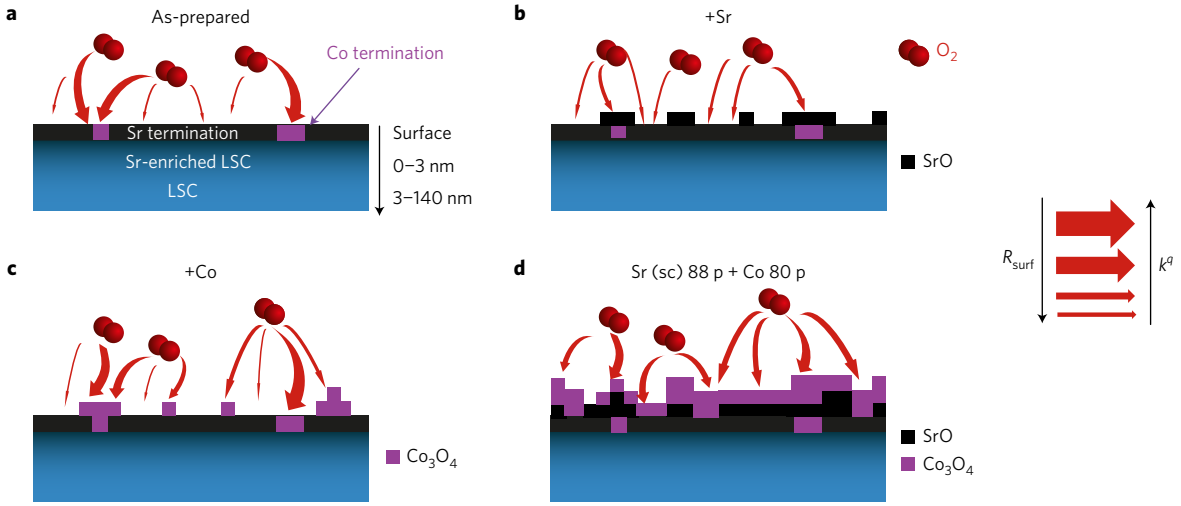

Figure 6 | Sketch of the model of inhomogeneously active LSC surfaces for the ORR. a, Sites of as-prepared thin films with Co termination (violet) show a higher exchange rate than regions with Sr termination (black). **b**, SrO causes an activity decrease (resistance increase). **c**, Co-oxide decoration leads to an increase of the ORR activity. **d**, The surface of a SrO decorated LSC electrode can be reactivated to its initial value by adding Co-oxides, provided the SrO layer is not too thick yet.

SrO layer, and this further enhances the polarization resistance. Either the rate-limiting step is still a surface-related oxygen dissociation/ionization step and electron transfer becomes more difficult for larger distances to 'buried' LSC sites, or ion transport through the SrO layer plays a role. This requires electronic and ionic conductivity of thin SrO layers, as recently proposed by Mogensen and colleagues[36]. This model may also explain the two slopes of the polarization resistance versus Sr amount plot (Fig. 4c): small 'Sr' amounts deactivate highly active sites and cause a larger slope, larger amounts 'only' thicken the SrO layer.

The effect of 'Co' decoration on an as-prepared LSC layer is similar to the effect of a removal of SrO by chemical etching[10]: in both cases more Co becomes available at the surface and thus the number of sites with fast oxygen exchange increases (see Fig. 6c). The positive effect of 'Co' might be limited by island formation, but also by the fact that oxygen vacancies are required for oxygen reduction, and those may be associated with Sr. Additional 'Co' on LSC with already existing SrO decoration can still strongly improve the oxygen exchange even though the underlying SrO hinders highest electrocatalytic activity (see Fig. 6d). The greater the amount of SrO deposited before 'Co' decoration, the higher the final resistance remains. Accordingly 'Co' is most active close to the LSC bulk.

In summary, these experiments show that small amounts of cations may matter a lot and that the high electrochemical activity of LSC is most probably caused by only few highly active (Co-based) sites at the surface. These insights could be gained by the novel technique of IPLD, which enables one to manipulate electrode surfaces while *in situ* measuring the ORR activity and thus avoids any alteration of the surface between preparation and investigation. The combination of PLD and impedance spectroscopy may not only be applicable to many other electrode surfaces but can also be highly valuable for directly monitoring the electrochemical properties of growing mixed ionic and electronic conducting thin films, even in the earliest stages. Hence, novel insights into the film thickness dependence of defect chemistry and ORR activity can be gained at an accuracy level not accessible so far.

Methods

Methods, including statements of data availability and any associated accession codes and references, are available in the online version of this paper.

Received 13 September 2016; accepted 13 February 2017; published online 27 March 2017

References

1. Boukamp, B. A. Fuel cells: the amazing perovskite anode. *Nat. Mater.* **2,** 294–296 (2003).
2. Choi, S. *et al*. Highly efficient and robust cathode materials for low-temperature solid oxide fuel cells: $PrBa_{0.5}Sr_{0.5}Co_{2-x}Fe_xO_{5+\delta}$. *Sci. Rep.* **3,** 2426 (2013).
3. Shao, Z. & Haile, S. M. A high-performance cathode for the next generation of solid-oxide fuel cells. *Nature* **431,** 170–173 (2004).
4. Rupp, G. M., Schmid, A., Nenning, A. & Fleig, J. The superior properties of $La_{0.6}Ba_{0.4}CoO_{3-\delta}$ thin film electrodes for oxygen exchange in comparison to $La_{0.6}Sr_{0.4}CoO_{3-\delta}$. *J. Electrochem. Soc.* **163,** F564–F573 (2016).
5. Baumann, F. S. *et al*. Quantitative comparison of mixed conducting SOFC cathode materials by means of thin film model electrodes. *J. Electrochem. Soc.* **154,** B931–B941 (2007).
6. Cai, Z., Kubicek, M., Fleig, J. & Yildiz, B. Chemical heterogeneities on $La_{0.6}Sr_{0.4}CoO_{3-\delta}$ thin films—correlations to cathode surface activity and stability. *Chem. Mater.* **24,** 1116–1127 (2012).
7. De Souza, R. A. & Kilner, J. A. Oxygen transport in $La_{1-x}Sr_xMn_{1-y}Co_yO_{3+/-\delta}$ perovskites—Part I. Oxygen tracer diffusion. *Solid State Ion.* **106,** 175–187 (1998).
8. Van der Haar, L. M., Den Otter, M. W., Morskate, M., Bouwmeester, H. J. M. & Verweij, H. Chemical diffusion and oxygen surface transfer of $La_{1-x}Sr_xCoO_{3-\delta}$ studied with electrical conductivity relaxation. *J. Electrochem. Soc.* **149,** J41–J46 (2002).
9. La O, G. J. *et al*. Catalytic activity enhancement for oxygen reduction on epitaxial perovskite thin films for solid-oxide fuel cells. *Angew. Chem. Int. Ed.* **49,** 5344–5347 (2010).
10. Rupp, G. M. *et al*. Surface chemistry of $La_{0.6}Sr_{0.4}CoO_{3-\delta}$ thin films and its impact on the oxygen surface exchange resistance. *J. Mater. Chem. A* **3,** 22759–22769 (2015).
11. Huber, A.-K. *et al*. *In situ* study of activation and de-activation of LSM fuel cell cathodes—electrochemistry and surface analysis of thin-film electrodes. *J. Catalys.* **294,** 79–88 (2012).
12. Wang, W. & Jiang, S. P. A mechanistic study on the activation process of (La, Sr)MnO_3 electrodes of solid oxide fuel cells. *Solid State Ion.* **177,** 1361–1369 (2006).
13. Hu, B., Mahapatra, M. K. & Singh, P. Performance regeneration in lanthanum strontium manganite cathode during exposure to H_2O and CO_2 containing ambient air atmospheres. *J. Ceram. Soc. Japan* **123,** 199–204 (2015).
14. Kubicek, M., Limbeck, A., Fromling, T., Hutter, H. & Fleig, J. Relationship between cation segregation and the electrochemical oxygen reduction kinetics of $La_{0.6}Sr_{0.4}CoO_{3-\delta}$ thin film electrodes. *J. Electrochem. Soc.* **158,** B727–B734 (2011).
15. Baumann, F. S. *et al*. Strong performance improvement of $La_{0.6}Sr_{0.4}Co_{0.8}Fe_{0.2}O_{3-\delta}$ SOFC cathodes by electrochemical activation. *J. Electrochem. Soc.* **152,** A2074–A2079 (2005).

16. Wang, H. *et al*. Mechanisms of performance degradation of (La,Sr)(Co,Fe)$O_{3-\delta}$ solid oxide fuel cell cathodes. *J. Electrochem. Soc.* **163,** F581–F585 (2016).
17. Oh, D., Gostovic, D. & Wachsman, E. D. Mechanism of $La_{0.6}Sr_{0.4}Co_{0.2}Fe_{0.8}O_3$ cathode degradation. *J. Mater. Res.* **27,** 1992–1999 (2012).
18. Chen, Y. *et al*. Impact of Sr segregation on the electronic structure and oxygen reduction activity of $SrTi_{1-x}Fe_xO_3$ surfaces. *Energy Environ. Sci.* **5,** 7979–7988 (2012).
19. Jung, W. & Tuller, H. L. Investigation of surface Sr segregation in model thin film solid oxide fuel cell perovskite electrodes. *Energy Environ. Sci.* **5,** 5370–5378 (2012).
20. Kim, Y.-M., Chen, X., Jiang, S. P. & Bae, J. Effect of strontium content on chromium deposition and poisoning in $Ba_{1-x}Sr_xCo_{0.8}Fe_{0.2}O_{3-\delta}$ ($0.3 \leq x \geq 0.7$) cathodes of solid oxide fuel cells. *J. Electrochem. Soc.* **159,** B185–B194 (2011).
21. Bucher, E., Gspan, C., Hofer, F. & Sitte, W. Sulphur poisoning of the SOFC cathode material $La_{0.6}Sr_{0.4}CoO_{3-\delta}$. *Solid State Ion.* **238,** 15–23 (2013).
22. Bucher, E., Sitte, W., Klauser, F. & Bertel, E. Impact of humid atmospheres on oxygen exchange properties, surface-near elemental composition, and surface morphology of $La_{0.6}Sr_{0.4}CoO_{3-\delta}$. *Solid State Ion.* **208,** 43–51 (2012).
23. Crumlin, E. J. *et al*. Oxygen electrocatalysis on epitaxial $La_{0.6}Sr_{0.4}CoO_{3-\delta}$ Perovskite thin films for solid oxide fuel cells. *J. Electrochem. Soc.* **159,** F219–F225 (2012).
24. Wilson, J. R., Sase, M., Kawada, T. & Adler, S. B. Measurement of oxygen exchange kinetics on thin-film $La_{0.6}Sr_{0.4}CoO_{3-\delta}$ using nonlinear electrochemical impedance spectroscopy. *Electrochem. Solid-State Lett.* **10,** B81–B86 (2007).
25. Baumann, F. S., Maier, J. & Fleig, J. The polarization resistance of mixed conducting SOFC cathodes: a comparative study using thin film model electrodes. *Solid State Ion.* **179,** 1198–1204 (2008).
26. Kawada, T. *et al*. Determination of oxygen vacancy concentration in a thin film of $La_{0.6}Sr_{0.4}CoO_{3-\delta}$ by an electrochemical method. *J. Electrochem. Soc.* **149,** E252–E259 (2002).
27. Tsvetkov, N., Lu, Q., Sun, L., Crumlin, E. J. & Yildiz, B. Improved chemical and electrochemical stability of perovskite oxides with less reducible cations at the surface. *Nat. Mater.* **15,** 1010–1016 (2016).
28. Yu, A. S., Küngas, R., Vohs, J. M. & Gorte, R. J. Modification of SOFC cathodes by atomic layer deposition. *J. Electrochem. Soc.* **160,** F1225–F1231 (2013).
29. Crumlin, E. J. *et al*. Surface strontium enrichment on highly active perovskites for oxygen electrocatalysis in solid oxide fuel cells. *Energy Environ. Sci.* **5,** 6081–6088 (2012).
30. Mutoro, E., Crumlin, E. J., Biegalski, M. D., Christen, H. M. & Shao-Horn, Y. Enhanced oxygen reduction activity on surface-decorated perovskite thin films for solid oxide fuel cells. *Energy Environ. Sci.* **4,** 3689–3696 (2011).
31. Kuhn, M., Hashimoto, S., Sato, K., Yashiro, K. & Mizusaki, J. Oxygen nonstoichiometry and thermo-chemical stability of $La_{0.6}Sr_{0.4}CoO_{3-\delta}$. *J. Solid State Chem.* **197,** 38–45 (2013).
32. Kubicek, M. *et al*. Cation diffusion in $La_{0.6}Sr_{0.4}CoO_{3-\delta}$ below 800 °C and its relevance for Sr segregation. *Phys. Chem. Chem. Phys.* **16,** 2715–2726 (2014).
33. Baumann, F. S., Fleig, J., Habermeier, H. & Maier, J. Impedance spectroscopic study on well-defined (La,Sr)(Co,Fe)$O_{3-\delta}$ model electrodes. *Solid State Ion.* **177,** 1071–1081 (2006).
34. Hjalmarsson, P., Søgaard, M. & Mogensen, M. Electrochemical performance and degradation of $(La_{0.6}Sr_{0.4})_{0.99}CoO_{3-\delta}$ as porous SOFC-cathode. *Solid State Ion.* **179,** 1422–1426 (2008).
35. Chen, Y. *et al*. Segregated chemistry and structure on (001) and (100) surfaces of $(La_{1-x}Sr_x)_2CoO_4$ override the crystal anisotropy in oxygen exchange kinetics. *Chem. Mater.* **27,** 5436–5450 (2015).
36. Mogensen, M. B. *et al*. New hypothesis for SOFC ceramic oxygen electrode mechanisms. *ECS Trans.* **72,** 93–103 (2016).
37. Maier, J. in *Physical Chemistry of Ionic Materials: Ions and Electrons in Solids* Ch. 7.3, 433–434 (John Wiley, 2004).

Acknowledgements

The authors gratefully acknowledge funding by Austrian Science Fund (FWF) project P4509-N16 and W1243-N16. Scanning electron microscope images were obtained using facilities at the University Service Centre for Transmission Electron Microscopy, Vienna University of Technology, Austria.

Author contributions

G.M.R. prepared the samples, developed the IPLD setup, performed and analysed impedance, X-ray diffraction and ICP measurements and wrote the manuscript. A.K.O. had the initial idea for the IPLD setup, supported the development and was involved at all stages of the study from planning to data analysis and discussion. A.N. performed XPS measurements and analysis. A.L. supervised the ICP measurements and was involved in the interpretation of the data. J.F. supervised all impedance spectroscopy measurements and was involved in the interpretation of the results as well as the preparation of the manuscript.

Additional information

Supplementary information is available in the online version of the paper. Reprints and permissions information is available online at www.nature.com/reprints. Publisher's note: Springer Nature remains neutral with regard to jurisdictional claims in published maps and institutional affiliations. Correspondence and requests for materials should be addressed to G.M.R.

Competing financial interests

The authors declare no competing financial interests.

Methods

Target preparation and characterization. The $La_{0.6}Sr_{0.4}CoO_{3-\delta}$ (LSC) target for pulsed laser deposition (PLD) was synthesized according to the Pechini route[38]. La_2O_3, $SrCO_3$ and Co powders (all Sigma Aldrich, 99.995%) were individually dissolved in nitric acid, mixed in appropriate ratios and citric acid (TraceSELECT, 99.9998%) was added for chelation. A calcination step was performed at 1,000 °C in air, followed by isostatic pressing (150 MPa) of the powder to a pellet and a sintering procedure at 1,200 °C for 12 h in air. The exact target composition ($La_{0.607\pm0.008}Sr_{0.396\pm0.004}Co_{0.996\pm0.005}O_{3-\delta}$) was determined from thin films grown by PLD on YSZ, which were dissolved in hydrochloric acid and analysed by inductively coupled plasma-optical emission spectroscopy. The $Ce_{0.8}Gd_{0.2}O_{2-\delta}$ (GDC) powder (Treibacher Industrie AG) was isostatically pressed (240 MPa) and sintered for 10 h at 1,550 °C in air to yield a PLD target. The 'La' and 'Sr' targets were prepared from La_2O_3 and SrO powders which were calcined in a platinum crucible at 800 °C and 1,200 °C, respectively, for 12 h in a constant flow of high-purity O_2 (ALPHAGAZ 1, >99.998 mol% oxygen) to decompose any hydroxyls or carbonates. After cooling down to room temperature in the same atmosphere, the powders were ground and isostatically pressed within an hour and the pellets sintered again at 1,200 °C ('La') and 1,300 °C ('Sr') for 12 h in a flux of high-purity O_2. For the 'Co' target, Co_3O_4 powder was ground, isostatically pressed and the pellet sintered at 1,200 °C for 12 h in ambient air. A SrO single crystal purchased from SurfaceNet (Rheine, Germany) was used as 'Sr (sc)' target. All targets were glued to target holders and the glue was cured at 180 °C for 4 h in a flux of high-purity O_2. All targets except from the LSC target were stored in a vacuum desiccator filled with silica gel (H_2O adsorbent) and freshly annealed SrO (H_2O & CO_2 getter) and transferred into the PLD immediately before evacuating the PLD recipient to avoid/reduce degradation of the materials.

The polycrystalline PLD targets were analysed in the Bragg–Brentano geometry by a X'Pert Powder (PANalytical) diffractometer. Diffraction patterns are shown in Supplementary Fig. 9 and allowed us to determine the phase compositions. For the 'Co' and 'La' target exclusively Co_3O_4 and La_2O_3 were found. For sake of simplicity particles deposited from the non-phase pure 'Sr' target (87 at% SrO, ∼10 at% $Sr(OH)_2$, ∼3 at% Sr_4PtO_6) were assumed to be pure SrO. The exact chemical composition of the deposited materials, however, was not accessible; it could be determined reliably only by a chemical *in situ* analysis in the PLD chamber. Although formation of hydroxides and carbonates is assumed to be unlikely inside the PLD chamber because of the high-purity oxygen used and the negligible nominal partial pressures of CO_2 and H_2O ($p_{CO_2} = 2.5 \times 10^{-10}$ bar and $p_{H_2O} = 1.5 \times 10^{-9}$ bar), *ex situ* XPS analysis of as-prepared and decorated thin films indicated the presence of hydroxyls and carbonates on the surface. It is assumed that LSC and the deposited oxides, especially SrO, react with moisture and CO_2 of the ambient atmosphere as soon as the samples are removed from the PLD recipient. Apart from this result, XPS measurements semi-quantitatively (Supplementary Fig. 5) confirmed the quantitative results found by ICP-MS.

Sample preparation. For the preparation of the samples, first dense ∼55 nm thin $Ce_{0.8}Gd_{0.2}O_{2-\delta}$ buffer layers and dense ∼140 nm thin LSC layers were deposited onto (100)-oriented yttria-stabilized zirconia (YSZ, 9.5 mol% Y_2O_3, Crystec GmbH, Germany) single crystals with a thickness of 0.5 mm and a size of $5 \times 5\,mm^2$. These layers were used as working electrodes of the electrochemical cells. Ablation of target materials was carried out by a KrF ($\lambda = 248$ nm) excimer laser (Lambda COMPexPro 201F) operated at a pulse repetition rate of 5 Hz, a pulse duration of 50 ns and a laser fluence of approximately $1.5\,J \cdot cm^{-2}$ at the target. The atmosphere was set to 4×10^{-2} mbar oxygen partial pressure (constant flux of high-purity O_2) and the substrate was heated to a surface temperature of 600 °C. About 1,500 and 6,750 laser pulses were applied to the GDC and LSC target, respectively, with a constant substrate to target distance of 6 cm. After deposition, the sample was cooled in the deposition atmosphere at a cooling rate of $12\,°C\,min^{-1}$. A cross-section of the WE of an as-prepared sample is shown in Supplementary Fig. 11. The substrate was flipped and a porous LSC counter electrode was prepared by PLD in 4×10^{-1} mbar oxygen partial pressure, at a substrate surface temperature of 450 °C, using 9,000 laser pulses and an adapted substrate to target distance of 5 cm. The morphological structure of such counter electrodes was analysed by transmission electron microscopy cross-sections; details on the electrochemical performance measured by impedance spectroscopy have been published in ref. 39.

Methods. The *in situ* impedance PLD (IPLD) setup is shown in Fig. 2. A corundum plate is placed on top of the uncovered Pt heating wires for electronic isolation. Next, a Pt sheet placed on top of the corundum plate is pinned down by a corundum ring (Fig. 1b); it is used to contact the counter electrode for the impedance measurement. A Pt wire wrapped around the entire length of a movable Cu arm was ground to a sharp (∼10 µm) tip at one end. It is fixed at an in-plane distance of 18 cm directly at a chamber feedthrough. Before putting a sample into the IPLD setup, targets were freshly ground, inserted into the PLD and ablated for 1 min in 5×10^{-1} mbar $p(O_2)$ at room temperature. Then, the PLD chamber was again opened and the sample was positioned on the Pt sheet directly below the target at a distance of 4.7 cm and the WE was contacted by manually placing the Pt tip of the Cu arm in the middle of the sample (see Fig. 1b). Subsequently, the chamber was evacuated and the atmosphere set to 5×10^{-1} mbar $p(O_2)$ before heating the sample to 450 °C. The temperature was controlled by measuring the ionic conductivity of the YSZ single crystal (see Supplementary Information). Figure 1a,c shows a photograph and a sketch of the entire system while applying one laser pulse onto a target. The surface area of the WE shadowed by the needle tip during material deposition amounts to 3–5%. This was estimated from microscope images (colour contrast) after growing a complete LSC electrode (∼150 nm) on top of YSZ. The laser repetition rate was set to 1 Hz for depositions using 1, 2, 5, 10, 20 and 50 laser pulses and increased to 2 Hz for ablations with 100, 200 or 500 laser pulses.

The impedance was measured by a Novocontrol Alpha A High Performance Frequency Analyzer in the frequency range from 10^6 to a minimum of 10^{-2} Hz with a resolution of five points per decade and an alternating voltage of 10 mV (rms) applied between the two thin film electrodes. The serial two-point Pt wire resistance (2–3 Ω at 450 °C) was separately measured by placing the tip of the WE contact directly on the Pt sheet. For each sample situation three spectra were measured subsequently, and those were generally in close agreement. This guarantees that resistance changes larger than 5–10%, found after surface decoration, are true effects and not caused by a parallel degradation process. Furthermore, continuous impedance measurements inside the PLD chamber for 6 h did not show any indication of electrode degradation, and the scatter of the surface exchange resistance of 4% was primarily because of temperature fluctuations (452 ± 3 °C; see Supplementary Fig. 3).

For the determination of the target deposition rates, 100, 500 and 1,000 laser pulses were used to ablate 'La', 'Sr', 'Sr (sc)' and 'Co' onto the surface of three YSZ single crystals, respectively, in a single run. The deposited materials were then dissolved in a 0.5 ml mixture of concentrated HCl, HNO_3 and H_2O_2 for over 16 hours. Afterwards, ∼14.5 ml of ultrapure H_2O and 15 µl of $10\,mg \cdot l^{-1}$ In (Indium Standard solution, Aristar) as internal standard were added to the clear solutions of dissolved cations. For quantification, a standard dilution series was prepared using a mixture of La (ICP-Multi-Element Standard, Aristar), Co and Sr (both Plasma EmissionStandard, Prolabor) in a similar acidic matrix. Analysis of standards and prepared sample digests was performed using quadrupole ICP-MS instrumentation (iCAP Qc, ThermoFisher Scientific, Bremen, Germany) equipped with an ESI SC-2DX autosampler. Introduction of prepared sample and standard solutions was accomplished using a concentric PFA nebulizer and a Peltier-cooled quartz spray chamber. Qtegra software provided by the manufacturer was used for data acquisition. Further details of ICP-MS analysis have been reported elsewhere[40]. Based on the cation concentrations determined for the sample digests the deposited cation amounts per laser pulse for the different target materials were calculated. Finally, the calibration curves presented in Supplementary Fig. 4 were calculated, showing the deposition rates achieved for the investigated LSC constituents. One may argue that the material ablated from the target by one pulse can lead to slightly different cation amounts on different substrates—that is, on YSZ (used for amount quantification) and LSC (used for impedance analysis). However, studies on different oxides revealed that such a substrate dependence of the deposition rate is approximately in the 5–15% range[41], and since the numbers of our laser pulses cover three orders of magnitude, these errors are of no importance.

XPS measurements were carried out on a spectrometer with monochromatic AlKα source (Microfocus 350, SPECS Surface Nano Analysis) and an angle-resolved photoelectron analyser (Phoibos WAL, SPECS), collecting photoelectrons in the range of 20 to 80° from the surface normal. Details on the experimental procedure and evaluation are given in Supplementary Information. The microstructure of the as-deposited and decorated LSC thin films was investigated by a FEI Quanta200 field emission gun scanning electron microscope equipped with an Everhart–Thornley detector at 5 kV accelerating voltage.

Data availability. The data that support the findings of this study are available from the corresponding author upon reasonable request.

References

38. Pechini, M. P. Method of preparing lead and alkaline earth titanates and niobates and coating method using the same to form a capacitor. US patent 3330697 A (1967).
39. Rupp, G. M. *et al*. Correlating surface cation composition and thin film microstructure with the electrochemical performance of lanthanum strontium cobaltite (LSC) electrodes. *J. Mater. Chem. A* **2,** 7099–7108 (2014).
40. Limbeck, A. *et al*. Dynamic etching of soluble surface layers with on-line inductively coupled plasma mass spectrometry detection—a novel approach for determination of complex metal oxide surface cation stoichiometry. *J. Anal. Atom. Spectr.* **31,** 1638–1646 (2016).
41. Kubicek, M. *et al*. Tensile lattice strain accelerates oxygen surface exchange and diffusion in $La_{1-x}Sr_xCoO_{3-\delta}$ thin films. *ACS Nano* **7,** 3276–3286 (2013).